Linking irradiance-induced changes in pit membrane ultrastructure with xylem vulnerability to cavitation

LENKA PLAVCOVÁ[1], UWE G. HACKE[1] & JOHN S. SPERRY[2]

[1]*Department of Renewable Resources, University of Alberta, Alberta, Canada T6G 2E3, and* [2]*Department of Biology, University of Utah, Salt Lake City, UT 84025, USA*

ABSTRACT

The effect of shading on xylem hydraulic traits and xylem anatomy was studied in hybrid poplar (*Populus trichocarpa* × *deltoides*, clone H11-11). Hydraulic measurements conducted on stem segments of 3-month-old saplings grown in shaded (SH) or control light (C) conditions indicated that shading resulted in more vulnerable and less efficient xylem. Air is thought to enter vessels through pores in inter-vessel pit membranes, thereby nucleating cavitation. Therefore, we tested if the ultrastructure and/or chemistry of pit membranes differed in SH and C plants. Transmission electron micrographs revealed that pit membranes were thinner in SH, which was paralleled by lower compound middle lamella thickness. Immunolabelling with JIM5 and JIM7 monoclonal antibodies surprisingly indicated that pectic homogalacturonans were not present in the mature pit membrane regardless of the light treatment. Porosity measurements conducted with scanning electron microscopy were significantly affected by the method used for sample dehydration. Drying through a gradual ethanol series seems to be a better alternative to drying directly from a hydrated state for pit membrane observations in poplar. Scanning electron microscopy based estimates of pit membrane porosity probably overestimated real porosity as suggested by the results from the 'rare pit' model.

Key-words: bordered pits; electron microscopy; homogenous pit membrane; phenotypic plasticity; plant water transport; xylem anatomy.

INTRODUCTION

In the majority of terrestrial plants, a large amount of water is lost by transpiration as stomata open to facilitate CO_2 uptake. The ability of plants to acquire and transport water to leaves is therefore an important factor, which often limits their productivity and survival (Sperry 2000; McDowell *et al*. 2008). Water transport in the xylem is driven by a gradient in negative pressure. Water columns are in a metastable state and are prone to being disrupted by the phenomenon of cavitation. Cavitation results in an embolized (air-filled) conduit, which is no longer available for water transport. According to the air-seeding hypothesis, cavitation occurs when air outside a water-filled conduit is aspirated into the conduit through pores in the cell wall. The pores will retain an air-water meniscus until the difference between the air pressure (P_a) and xylem pressure (P_x) exceeds a critical pressure difference (ΔP_{crit}), according to:

$$\Delta P_{\mathrm{crit}} = \frac{4T \cos \alpha}{D_p} \qquad (1)$$

where $\Delta P = P_a - P_x$, T is the surface tension of xylem sap and α is the contact angle between sap and pore wall material, which is usually assumed to be zero (i.e. total wetting). The value of ΔP_{crit} is inversely related to the pore diameter (D_p). The largest pores in conduit walls appear to be located in the pit membranes that permit water flow between conduits (Sperry & Tyree 1988; Cochard, Cruiziat & Tyree 1992; Sperry *et al*. 1996). The air-seeding threshold is therefore determined by the structure of pit membranes, and pits represent a weak link in the protection of the transpiration stream against air entry (Choat, Cobb & Jansen 2008).

Cavitation resistance can vary even within a species or genotype in response to factors such as water status (e.g. Stiller 2009), nitrogen fertilization (Hacke *et al*. 2010), and shading (Cochard, Lemoine & Dreyer 1999). Lower irradiance is usually associated with lower evaporative demand and stomatal conductance, which is paralleled by a decreased need for water transport. Hence, xylem-specific and leaf-specific conductivity tend to be lower in shade (Shumway, Steiner & Kolb 1993; Caquet *et al*. 2009). The risk of drought-induced embolism is also usually lower in shade environments, implying reduced requirements for xylem safety. As a result, the xylem might be more vulnerable as the safety features are costly and shaded plants have limited carbon resources, which are preferentially allocated to promote light capture (Schoonmaker *et al*. 2010). Indeed, the majority of studies found increased vulnerability as a result of shading (Cochard *et al*. 1999; Barigah *et al*. 2006; Schoonmaker *et al*. 2010). However, others found no change (Raimondo *et al*. 2009) or increased resistance (Holste, Jerke & Matzner 2006) in shaded plants. Thus, there is still some ambiguity in the effect of light on cavitation resistance.

The main objective of this study was to evaluate the effect of contrasting light availability on cavitation resistance and on the ultrastructure of inter-vessel pits in poplar

Correspondence: U. G. Hacke. Fax: +780 492 1767; e-mail: uwe.hacke@ualberta.ca

xylem. Based on previous findings (see earlier) and considering the potential of poplar xylem for phenotypic plasticity (Hacke *et al.* 2010) we expected that shaded plants will be more vulnerable to cavitation. Given the central role of inter-vessel pits in determining cavitation resistance, we expected to find larger pores in the pit membranes of shaded plants. Observations of homogeneous pit membranes in angiosperm species showed significant variation in their structure (Jansen, Choat & Pletsers 2009), and correlations between ΔP_{crit} and pore size as well as pit membrane thickness have been observed. However, the potential for structural acclimation at the pit membrane level within a single angiosperm species or genotype remains to be evaluated. A certain degree of phenotypic plasticity in the structure and function of inter-vessel pits can be expected as acclimation at the pit level has already been described in conifers (Domec *et al.* 2008; Schoonmaker *et al.* 2010).

In order to test our hypothesis we used scanning (SEM) and transmission electron microscopy (TEM). Both methods have often been used to study pit membrane ultrastructure (e.g. Schmid & Machado 1968; Sano 2005; Jansen *et al.* 2009) even though there are valid concerns that artefacts caused by sample preparation may occur. This is especially true for SEM during which the delicate pit membranes are not supported by any embedding medium (Jansen, Pletsers & Sano 2008). Previous studies relating measured pit membrane pore sizes to the corresponding air-seeding pressure have reinforced these concerns. In at least two cases, membrane pores were much smaller than pores that would allow air-seeding at realistic xylem pressures (Shane, McCully & Canny 2000; Choat *et al.* 2003). It has been proposed that the large pores that allow air-seeding are very rare and therefore not likely to be detected with SEM (Hargrave *et al.* 1994; Wheeler *et al.* 2005; Choat *et al.* 2008). This concept is also known as the 'rare pit' hypothesis. Recently, Christman, Sperry & Adler (2009) developed a model that allows predicting the frequency of pits with a certain porosity based on stem-level air-seeding experiments. Here we used this model to test how pit porosity data observed with SEM agree with measured proxies of cavitation resistance. The pit membrane structure of poplars is particularly suitable for this approach, because membranes bear many large, easily resolvable pores (Jansen *et al.* 2009).

Pit membranes may also differ in their chemical composition. It is difficult to elucidate what chemical compounds are present in the pit membrane considering the small size of pit membranes and the fact that their surface is usually obscured by an overarching secondary cell wall. It is generally assumed that their chemical nature is similar to that of the primary cell wall from which the pit membranes are derived. Pectins, and specifically their subgroup homogalacturonans (HG), are believed to be important components of pit membranes (Zwieniecki, Melcher & Holbrook 2001; Cochard *et al.* 2010). HG can differ in the degree of methyl-esterification, which has consequences for the flexibility and extensibility of the primary cell wall (Goldberg, Morvan &

Roland 1986; Guglielmino *et al.* 1997; Willats *et al.* 2001). The flexibility of pit membranes might influence the vulnerability to cavitation as pores may enlarge when pit membranes deflect during the process of air-seeding (Choat *et al.* 2004; Cochard *et al.* 2010). We therefore asked whether plants growing under contrasting light levels differed in the abundance of pectins and/or the degree of their esterification by using monoclonal antibodies, JIM5 and JIM7, which recognize HG with low and high degrees of methyl-esterification, respectively (Knox *et al.* 1990).

Saplings of hybrid poplar were grown under contrasting irradiance for 6 weeks. The resulting changes in xylem traits were assessed with light and electron microscopy as well as physiological measurements. Our main hypothesis was that shaded saplings will exhibit increased vulnerability to cavitation along with larger pores in their pit membranes. Differences in light level can have a profound effect on other aspects of hydraulic architecture, including conduit size and transport efficiency (Schoonmaker *et al.* 2010). Our second hypothesis was that decreased evaporative demands will correspond with narrower vessels and lower xylem area-specific and leaf-specific conductivities in shaded plants. As carbon resources tend to be more limited in shaded plants, we finally expected that xylem cells of shaded plants will exhibit thinner cell walls and lower wood density than in plants growing at higher light level.

METHODS

Plant material and sampling strategy

Seedlings of hybrid poplar (*Populus trichocarpa × deltoides*, clone H11-11) were produced from rooted cuttings. The seedlings were maintained in a growth chamber from December 2008 to February 2009 under a 16/8 h day/night cycle, 24/18 °C day/night temperature, and a daytime relative humidity of 75%. Plants were kept in 6 L pots filled with standard gardener soil and fertilized once a week with 500 mL of a complete water soluble fertilizer (20–20-20 N-P-K, Plant Products, Brampton, Ontario, Canada) in 1 g/L dilution. After 8 weeks of sapling establishment, shading structures were built over 11 randomly selected plants. The shading resulted in 80% reduction in irradiance from 350 μmol m^{-2} s^{-1} [control (C)] to 70 μmol m^{-2} s^{-1} [shade (SH)]. Plants were harvested 6 weeks after the beginning of the shade treatment. Hydraulic measurements and silicone injections for vessel length measurements were conducted within 4 days after harvesting. For these measurements 25 cm long stem segments were cut from the basal part of the plant (7 cm above the root collar). After the hydraulic measurements were completed, stem segments were stored at –4 °C and later used for vessel diameter and wood density measurements.

Vulnerability to cavitation, xylem and leaf specific conductivity

Stem segments trimmed to a final length of 14.2 cm were used to generate vulnerability curves. The hydraulic

conductivity of the stems was measured using a method originally described in Alder *et al*. (1997). Briefly, a filtered (0.2 μm) measuring solution (20 mM KCl + 1 mM CaCl$_2$) was perfused through stem segments under a pressure head of 4–5 kPa. Flow through the segments was recorded with an electronic balance (CP225D, Sartorius, Göttingen, Germany), which was interfaced with a computer. Maximum hydraulic conductivity (K_{max}) was determined after flushing the segments for 15 min at 50 kPa. Xylem area-specific conductivity (K_S) and leaf-specific conductivity (K_L) were calculated by dividing K_{max} by cross-sectional xylem area and leaf area distal to the measured segment, respectively (Tyree & Zimmermann 2002). Vulnerability curves were generated by spinning segments in a centrifuge to progressively more negative pressure and measuring the loss of hydraulic conductivity at each pressure. After fitting the curves to a Weibull function, cavitation resistance was expressed as the mean cavitation pressure (*MCP*). The *MCP* is the mean of the Weibull probability density function. In perfectly sigmoidal curves, the *MCP* equals the xylem pressure associated with 50% loss of hydraulic conductivity (*P50*). Six stems per group were measured for each light treatment.

TEM and immunolabelling of pectin epitopes

TEM was used to study the effect of light level on pit membrane thickness, cell wall thickness and on the presence and distribution of HG in cell walls and pit membranes. For the regular TEM, small blocks of xylem tissue (1 × 1 × 2 mm) were fixed overnight at room temperature in a fixative containing 2% paraformaldehyde and 2.5% glutaraldehyde in 0.05 M phosphate buffer. The following day, samples were repeatedly buffer-washed, postfixed in osmium tetroxide for 2 h, 3× buffer-washed and dehydrated in a graded ethanol series (20–30-40–60-80–90-100–100% for 15 min each). The dehydrated samples were embedded in Spurr resin. Ultrathin sections (80 nm) were sectioned with an ultramicrotome (Ultracut E, Reichert-Jung, Vienna, Austria), collected on copper grids and contrasted in uranyl acetate and lead citrate.

Immunolabellling with JIM5 and JIM7 antibodies, kindly donated by Prof J.P. Knox (University of Leeds, UK), was used to detect pectic HG in xylem samples. JIM5 and JIM7 are well-characterized monoclonal antibodies that have been previously used to detect differently-esterified HG in various plant tissues (Guglielmino *et al*. 1997; Hafren & Westermark 2001; Guillemin *et al*. 2005). Typically, JIM5 binds to HG with few or no esters, whereas JIM7 recognizes highly methyl-esterified pectin epitopes (Knox *et al*. 1990). In our experiment, we followed a preparation procedure described by Micheli *et al*. (2002). After fixation in 4% paraformaldehyde and 1.25% glutaraldehyde in 0.05 M phosphate buffer for 1.5 h at room temperature, samples were dehydrated in an ethanol series as described earlier. Samples were then embedded in LR White resin. Ultrathin sections collected on nickel grids were immunolabelled by floating the grids on drops of successively changing solutions. Sections were preincubated for 10 min on a drop of 0.05 M Tris-buffered saline (pH = 7.6) with 0.1% Tween 20 and 0.1% bovine serum albumin, blocked for 20 min with goat serum (Sigma-Aldrich Corp., St. Louis, MO, USA) diluted 1:30 (v/v) in the same buffer, treated with the primary antibody JIM5 or JIM7 (diluted 1:45) for 4 h, four times buffer-washed and stained with a secondary antibody, goat-anti rat IgG conjugated with 10 nm gold particles (Sigma-Aldrich Corp.) for 1 h. The grids were then extensively washed with buffer and filtered water and finally contrasted with 1% uranylacetate for 25 min. All these steps were conducted at room temperature.

Regular and immunolabelled samples were examined under a transmission electron microscope (Morgagni 268, Fei Company, Hillsboro, OR, USA). About 20 individual pit membranes from five individual stems were photographed at 20 000–45 000× magnification and used for pit membrane thickness measurements in both light treatments. For cell wall thickness measurements, a region of a vessel and a fibre adjacent to each other was randomly selected and photographed. The thickness of the electron dense compound middle lamella (a layer composed of the middle lamella and primary cell walls of two adjacent cells) was measured together with the thickness of the less electron dense secondary cell wall of fibres and vessels. Five different vessel-fibre regions were measured in each stem; five stems were measured in total for each light treatment. Three grids were prepared for immunostaining with each antibody for both SH and C samples.

SEM

Two sample preparation procedures were used to generate samples for SEM. Initially, fresh stem segments 1.5 cm in length were air-dried on a bench for several weeks. Samples were split longitudinally with a razor blade and mounted on aluminum stubs using conductive silver paste. The split was made about 1 mm from the surface of the stem to expose pits that developed under treatment conditions. Although air-drying without any chemical treatment was recently recommended for observing pit membranes (Jansen *et al*. 2008), we experienced difficulties finding undamaged pits in our plant material. We attributed this to the capillary forces caused by the high surface tension of water. Therefore, we gradually exchanged water for pure ethanol (with low surface tension) before air drying the samples. Frozen stem samples were thawed and soaked for 5 days in distilled water. Samples were subsequently dehydrated through an ethanol series (30–50-70–90%) for 30 min in each solution, immersed in 100% ethanol overnight, and finally air-dried. Splitting and mounting was conducted as described earlier. Samples were sputter coated with chromium and carbon. The thickness of the coating was approximately 5–10 nm. Samples were observed with a field-emission scanning electron microscope (6301F, JEOL, Tokyo, Japan) under 2 kV accelerating voltage. Pictures of pit membranes were taken at 8000–15 000× magnification. In shade samples prepared by air-drying from water it was difficult to find undamaged

exposed membranes. Therefore, about 15% of pictures were taken through the aperture in the secondary cell wall in these samples. In the rest of the images, at least half of the fully exposed membrane area was analysed to provide a reliable estimate of pit membrane porosity. Pore size was measured using image analysis software (ImagePro Plus version 6.1, Media Cybernetics, Silver Spring, MD, USA). Pore areas were converted into diameters assuming a circular shape of pores. Pores smaller then 20 nm in diameter could not be accurately distinguished from random pixel noise and were excluded. Maximum (D_{max}) and average pore size (D_{mean}) were determined for each pit membrane. About 100 individual pit membranes from at least 30 different pit fields were measured for each light treatment and each preparation technique. Individual pit-level measurements were averaged for each stem segment analysed.

'Rare pit' model

Details of the model have been described previously (Christman *et al.* 2009). According to the air-seeding hypothesis, the cavitation threshold for a given vessel is determined by the size of the largest pore that can be present in any of the pits in the vessel. An assumption of the rare pit hypothesis is that there are few pits with large pores and with relatively low air-seeding pressure, compared with the majority of 'air-tight' pits. A cumulative distribution function (cdf) $F_m(p)$ can be used to describe the cumulative frequency of inter-vessel pits that air seed at progressively greater pressure difference (p). Assuming that pits are independently distributed among vessel endwalls, the $F_m(p)$ can be used to calculate the cumulative frequency of vessel end walls that air seed at increasing pressure differences [end wall cdf, $F_e(p)$]:

$$F_e(p) = 1 - [1 - F_m(p)]^u \qquad (2)$$

where u is the number of inter-vessel pits per vessel. The $F_e(p)$ cdf can be converted into the corresponding probability density function (pdf). The mean pressure of this distribution represents the mean end wall air-seeding pressure (MCP_e). This value should be a proxy for the MCP of the xylem.

From SEM porosity measurements, we obtained empirical $F_m(p)$ distributions. Firstly, the Young-Laplace equation (Eqn 1) was used to convert the D_{max} of individual pits to the corresponding air-seeding pressure (P_a). Secondly, the empirical data were fitted with a Weibull cdf

$$F_m(p) = 1 - e^{-(p/b)^c} \qquad (3)$$

where b is the scale, and c is the shape fitting parameter of the Weibull distribution. Then, we used the fitted distribution $F_m(p)$ in Eqn 2 to calculate MCP_e. Initial calculations based on D_{max} yielded high (less negative) MCP_e in comparison with the measured MCP. It is likely that dehydration of the membranes resulted in enlargement of the pit pores from their native state because of shrinkage of the

membrane matrix. To account for this, we also represented the D_{max} per pit by averaging the top percentile of pore diameters per pit, and finding the percentile that provided the best fit of MCP_e to MCP.

Xylem anatomy

Stem cross-sections were prepared with a sliding microtome (SM2400, Leica Microsystems, Wetzlar, Germany) from the centre of segments previously used for hydraulic measurements. The sections were stained with toluidine blue for 3 min, rinsed in water, mounted on slides and observed with a light microscope (DM3000, Leica). Three radial transects were selected in a cross-section. Images were captured with a digital camera (DFC420C, Leica). The diameters (D) of vessels in each radial sector were measured using image analysis software (ImagePro). The hydraulic diameter (D_h) was then calculated as $D_h = (\Sigma D^5)/(\Sigma D^4)$. A total of 300 to 500 vessel diameters was measured per stem; six stems were analysed for each light treatment. The vessel double wall thickness (t_h) was measured on vessel pairs in which at least one of the vessels fell within $\pm 3 \mu$m of D_h. A total of 15 vessel pairs was measured per stem; six stems were analysed for each light treatment.

Vessel length was measured using the silicone injection method (Sperry, Hacke & Wheeler 2005). Stems 14 cm in length were flushed for 15 min at 50 kPa. Silicone (Rhodorsil RTV-141, Bluestar Silicones, distributed by Skycon, Toronto, Ontario, Canada) was mixed with a fluorescent whitening agent (Uvitex OB, Ciba Specialty Chemicals, Tarrytown, NY, USA), and injected into the stems at a pressure of 50 kPa for 24 h. The silicone did not penetrate vessel end walls. Therefore, a progressively decreasing number of vessels was filled with silicone as the distance from the injection surface increased. This relationship can be fitted with an exponential decay function, and the vessel length distribution can be estimated. The mean of log-transformed vessel length data (L) was used to represent the vessel length distribution of a stem. Five to six stems per light treatment were analysed. Vessel element length as well as the length and diameter of wood fibres were measured on macerated wood tissue, using a light microscope and image analysis software. At least 100 cells were measured from each individual stem; six stems were analysed for each light treatment. The number of pits per vessel, the u parameter of the rare pit model, was calculated as the total pit membrane area per vessel (A_p) divided by the area of individual pit membranes (A_i). To measure A_i longitudinal sections of stem xylem were prepared and observed under 1000× magnification. The A_p was estimated as the product of average vessel area (A_v), contact fraction and pitfield fraction (see details in Wheeler *et al.* 2005).

Wood density

Wood density (ρ) was determined on six segments per group by water displacement. Debarked stem segments approximately 2 cm in length were split longitudinally and

Table 1. Growth characteristics of poplar saplings grown under shade (SH) or control light conditions (C)

	Height (cm)	D_{stem} (mm)	LA_{total} (m^2)	DW_{leaf} (g)	LMA (g/m^2)	LA/XA (cm^2/mm^2)
SH	115.7 ± 6.0	6.7 ± 0.2	0.47 ± 0.04	19.7 ± 1.5	41.9 ± 1.2	211.4 ± 8.3
C	108.4 ± 3.2	8.1 ± 0.2	0.50 ± 0.02	34.3 ± 1.0	69.9 ± 3.4	170.3 ± 15.7
P value	0.001	<10^{-3}	ns (0.341)	<10^{-3}	<10^{-3}	<10^{-3}

Parameters shown are sapling height (*height*), stem diameter (D_{stem}) at 10 cm above the root collar, total leaf area (LA_{total}), total leaf dry mass (DW_{leaf}), leaf mass per unit leaf area (LMA) and supported leaf area (LA) to xylem area (XA) ratio of the measured stem segment. Means ± standard deviation, $n = 6$–12. P values show results of independent two-sample t-tests, testing for differences between the two light treatments; ns = non-significant difference.

the pit was removed. Samples were submersed in a beaker of water on a balance to determine the fresh volume of wood. Samples were then oven-dried at 70 °C for 48 h. Wood density of each sample was calculated as $\rho =$ dry weight/ fresh volume.

Statistics

Prior to the analysis, normality and homogeneity of variance were graphically checked. Independent two sample *t*-tests were used to compare the differences in means between SH and C. Two-way analysis of variance (ANOVA) and Tukey's honestly significant difference (HSD) *post hoc* comparison tests were used to dissect the effect of light treatment and sample preparation technique on porosity data. The statistical software package R 2.10.1 (R Development Core Team 2009, Auckland, New Zealand) was used to perform the analysis.

RESULTS

Plant growth

Hybrid poplar is a fast growing tree with a high demand for light. When shaded, the saplings exhibited a typical response of shade avoiders. They enhanced shoot elongation and developed thinner leaves in order to increase light interception (Table 1). Average daily height increments were 2.2 ± 0.1 and 2.0 ± 0.1 cm [mean ± standard deviation (SD)], leading to a final height of 115.7 ± 6.0 and 108.4 ± 3.2 cm in SH and C plants, respectively. The radial growth of SH plants was reduced, which resulted in thinner stems in this plant group ($D_{stem} = 6.7 \pm 0.2$ versus 8.1 ± 0.2 mm in SH and C plants, respectively). Total leaf area (LA_{total}) was the same, but leaf dry mass was much larger in C plants implying a strong difference in leaf mass per unit leaf area (LMA). For the stem segments used for hydraulic measurements, the ratio between supported leaf area and cross-sectional xylem area (LA/XA) was significantly higher in SH plants.

Xylem vulnerability and hydraulic conductivity

Differences in light level had an effect on vulnerability of stems to cavitation (Fig. 1a). SH plants were more vulnerable with a MCP of −1.13 ± 0.10 MPa, compared with −1.51 ± 0.06 MPa in C stems. In addition to being more resistant to cavitation, stems of C plants showed higher transport efficiency than those of SH plants. The specific conductivity values (K_S) were 6.6 ± 0.6 and 4.7 ± 0.4 kg s^{-1} m^{-1} MPa^{-1} in C and SH stems, respectively (Fig. 1b). Leaf-specific conductivity was almost twice as high in C plants (Fig. 1c).
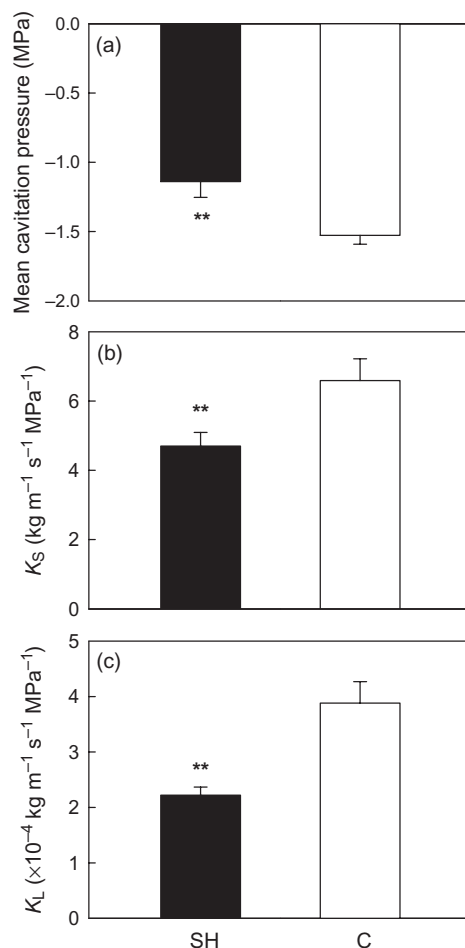

Figure 1. Mean cavitation pressure (a), xylem-area specific (b), and leaf-specific (c) conductivity of stem segments from poplar saplings grown under shade (SH; black bars) or control light conditions (C; open bars). Error bars show standard deviation ($n = 6$). ** indicates significant differences at $P < 0.01$ (independent two-sample t-test).
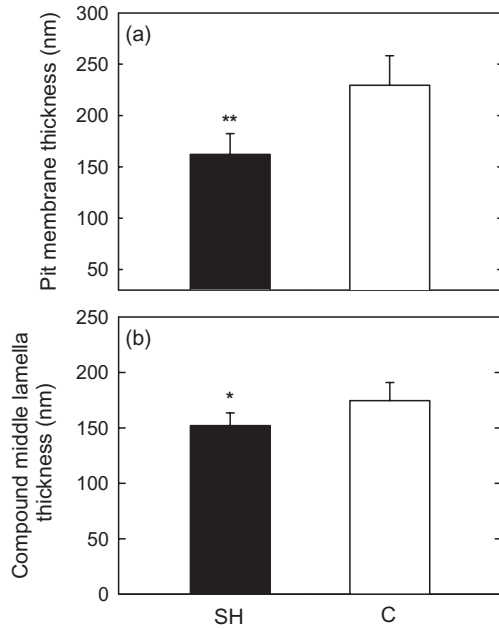
Figure 2. Pit membrane (a) and compound middle lamella (b) thickness in plants grown in shade (SH; black bars) or control light conditions (C; open bars). The bars represent grand means ± SD ($n = 5$). * and ** indicate significant differences at $P < 0.05$ and 0.01, respectively (independent two-sample t-test).

Pit membrane ultrastructure and immunolabelling

TEM micrographs revealed that inter-vessel pit membranes in SH plants were thinner (162.1 ± 20.3 nm) than in C plants (229.5 ± 28.8 nm) (Fig. 2a). Differences in pit membrane thickness were paralleled by a similar trend in compound middle lamella thickness (Fig. 2b). Pit membranes appeared granular and less electron-dense than the adjacent compound middle lamella layer (cml). The annulus (the periphery of the pit membrane) was usually more electron-dense than the rest of the pit membrane, and could clearly be distinguished at the transition between primary cell wall and the actual pit membrane (Fig. 3b).

The immunolocalization pattern for both antibodies, JIM5 and JIM7, was similar in SH and C xylem. JIM7 provided a slightly stronger signal than JIM5. The distribution of immunogold particles indicated that HG were present in the compound middle lamella. The strongest labelling was found in cell corners (Fig. 3a). Most importantly, neither JIM5 nor JIM7 labelling were evident in the pit membranes, with an exception of the annulus, which often showed stronger labelling than seen in the compound middle lamella (Fig. 3b).

In SEM micrographs, resolvable pores were observed in the vast majority of pit membranes, but their number and size varied substantially. Measurements of membrane porosity gave contrasting results depending on the sample preparation method. In water-dried samples (air-dried from water), pores appeared to be larger than in ethanol-dried samples (air-dried from pure ethanol). Drying from water
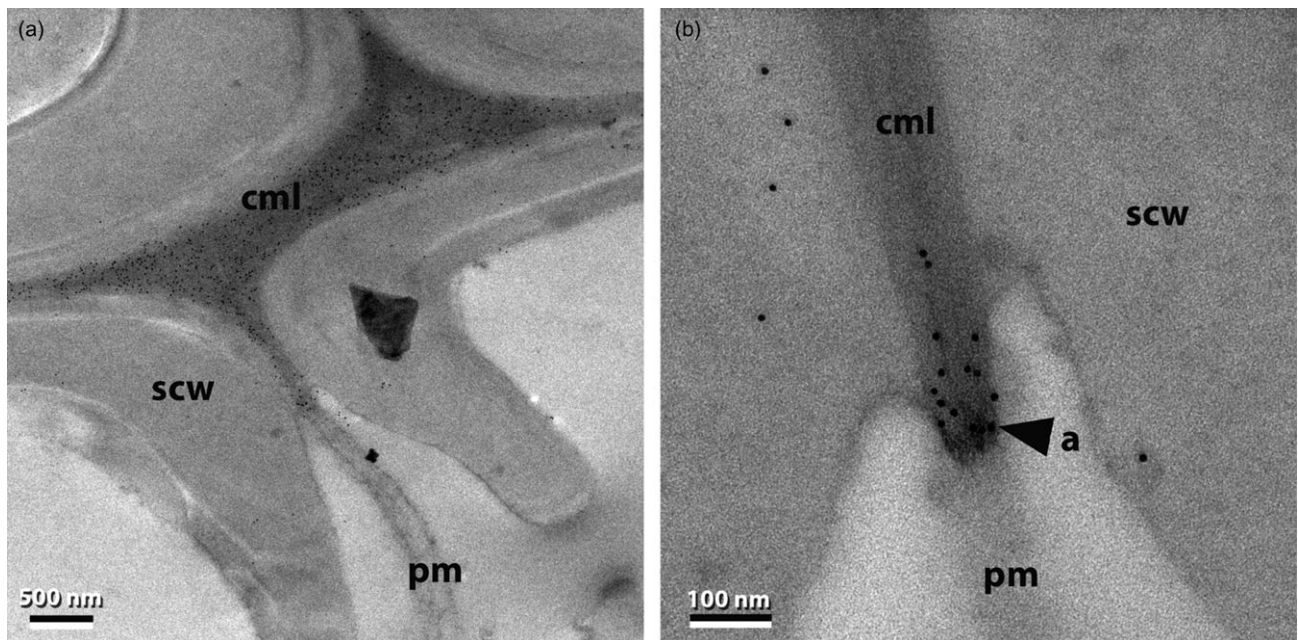

Figure 3. Immunogold localization of homogalacturonans in mature xylem with the monoclonal antibody JIM7 with transmission electron microscopy. JIM7 labelled the compound middle lamella (cml), but not the mature pit membrane (pm), indicating that homogalacturonans were not present in the pm (a). Gold particles were frequently located in the pit membrane annulus (arrowhead marked 'a') (b). Plants were grown in shade (a) and control light conditions (b).

tended to produce a high number of pit membranes with a non-microfibrilous texture and large, round and well-defined pores (Fig. 4a). In contrast, the surface of ethanol-dried pit membranes usually displayed an extensive meshwork of randomly oriented microfibrils connected with amorphous filling material. The pores were generally smaller and not as clearly distinguishable as in water-dried samples (Fig. 4b). In a few instances, pit membranes with no visible pores were observed and such membranes also lacked a resolvable microfibrilous texture. In some cases, a gelatinous layer was observed. This layer seemed to be detached along the edges of the pit membrane, thereby forming a distinct white ring (Fig. 4c).

The influence of the drying method on pore size was more pronounced in the thinner pit membranes of SH samples (Fig. 5). The maximal pore diameter per pit (D_{max}), the mean diameter of the largest 10% of pores per pit ($D_{10\%}$), and the mean pore diameter per pit (D_{mean}) were all significantly larger in water-dried samples than in ethanol-dried SH samples (compare black and grey bars on the left hand side of Figure 5a-c). In water-dried samples, all measures of pore size tended to be larger in SH than in C plants. By contrast, in ethanol-dried samples, pore size did not vary in response to light level (Fig. 5, compare grey bars).

'Rare pit' model

Given the fact that the different preparation techniques had a larger effect on pit porosity than the light treatments, we pooled SH and C data while distinguishing between ethanol- and water-dried samples when calculating the expected MCP (MCP_e) using the rare pit model. For both preparation methods, the predicted MCP_e was substantially higher (less negative) than the value obtained from vulnerability curves when D_{max} was used (Fig. 6a,b, solid thick curves). In ethanol-dried samples, a reasonable agreement between modelled and measured MCP was found when averages of the largest 7.5% of pores were used instead of the single largest pore diameters (Fig. 6a, dashed curve). In water-dried samples, the best agreement between modelled and measured MCP was achieved when the average of
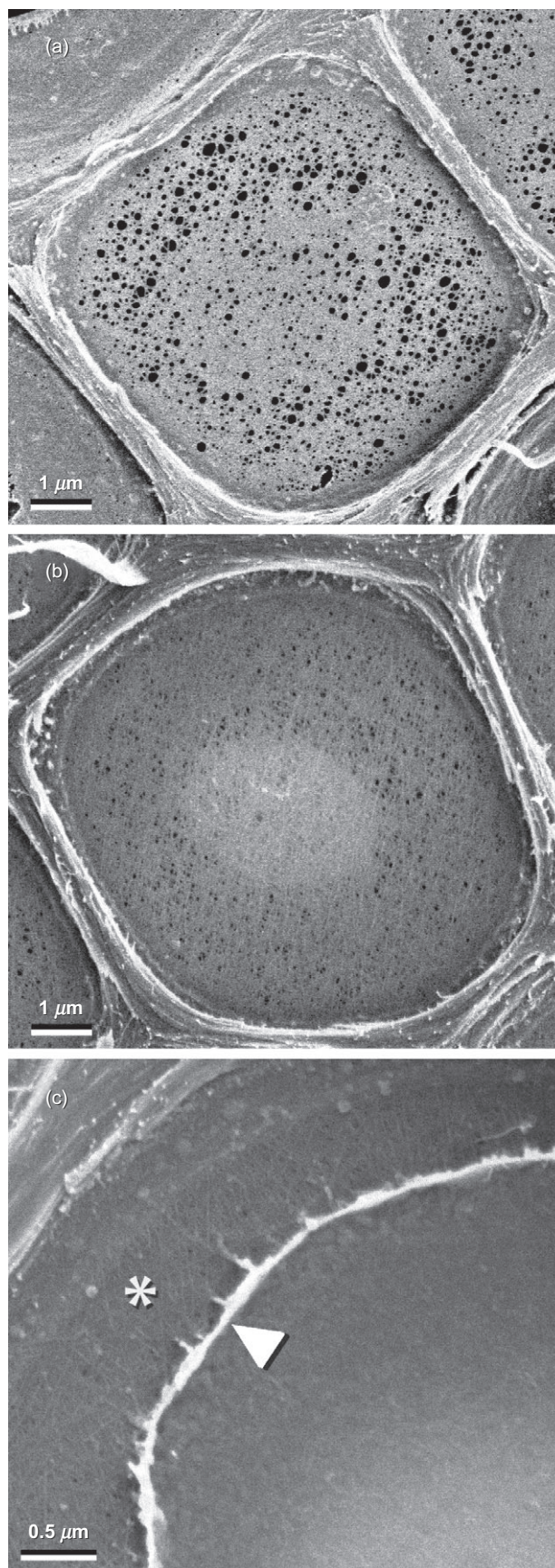

Figure 4. Scanning electron micrographs of exposed pit membranes. Porosity and texture of the pit membranes differed depending on the drying method used for sample preparation. Pit membranes from water-dried (i.e. air-dried from the fully hydrated state) samples (a) displayed large clearly resolvable pores and no visible microfibrils. Pit membranes from ethanol-dried samples (b) showed smaller pores embedded in a readily visible meshwork of randomly oriented microfibrils. The outline of the pit aperture is apparent as a lighter area in the centre of the pit membrane. Close-up view of the pit membrane (c) showing amorphous material (arrowhead) being detached from the edges of the pit membrane revealing a layer with visible pores and microfibrils (asterisk). The pictures were taken in samples from shaded plants (a, b) and plants grown under control light conditions (c).
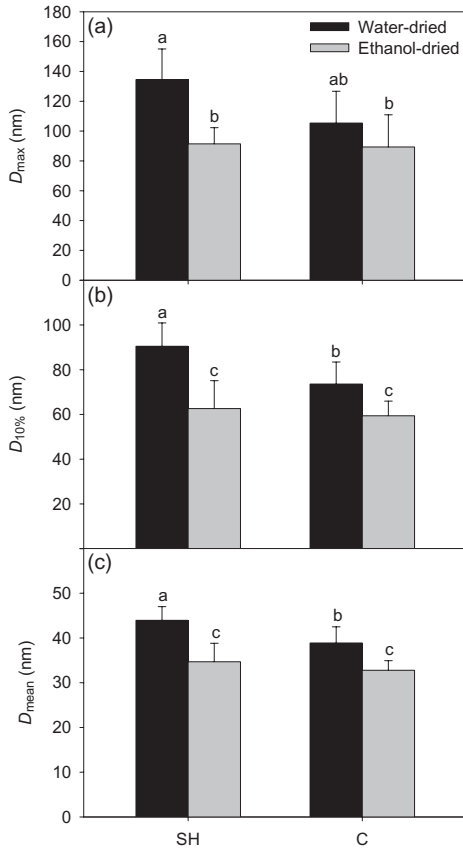
Figure 5. Scanning electron microscopy (SEM)-based measurements of pit membrane porosity. Maximal pore diameter D_{max} (a), average diameter of the 10% largest pores $D_{10\%}$ (b), and mean pore diameter D_{mean} (c) measured per pit in water-dried (black bars) or ethanol-dried (grey bars) SEM samples. The bars represent grand means ± standard deviation from six individual stems. Bars with no letters in common were statistically different at $P < 0.05$ (two-way analysis of variance and Tukey's honestly significant difference test).

the largest 50% of pores was used (Fig. 6b). The Weibull parameters for cumulative pit frequency distributions and the corresponding MCP_e predicted by the model for various pit porosity data are presented in Table 2.

Vessel and fibre anatomy

Shading resulted in significant changes in the dimensions of xylem cells. Vessels in SH stems were narrower (Fig. 7a) and longer (Fig. 7b) than in C stems. Hydraulic vessel diameters were 41.1 ± 1.2 and $43.1 \pm 1.4\,\mu m$ in SH and C plants, respectively. Mean vessel lengths were 3.9 ± 0.4 cm in SH and 3.1 ± 0.2 cm in C stems. The increased length of vessels in SH plants was in agreement with a higher average vessel element length ($238.5 \pm 10.8\,\mu m$ in SH versus $226.3 \pm 7.2\,\mu m$ in C) (Fig. 7c). Secondary cell wall thickness of vessels measured from TEM micrographs did not significantly differ between SH and C plants although the wall tended to be thinner in SH plants (Fig. 8a). The double

vessel wall thickness measured with light microscopy was significantly lower in SH than in C plants (Fig. 8b). While fibre diameters did not change in response to light level, fibre length was significantly reduced in SH plants (Table 3). Analysis of TEM images showed that shading also resulted in significantly thinner secondary cell walls in fibres, a trend that was paralleled by lower wood densities in stems of SH plants (Table 3).

DISCUSSION

In agreement with our main hypothesis, hybrid poplar saplings exhibited increased xylem vulnerability when grown under shade (Fig. 1a). This finding is consistent with previous results on other tree species (Cochard *et al.* 1999; Barigah *et al.* 2006; Schoonmaker *et al.* 2010). Increased vulnerability was associated with thinner pit membranes. This
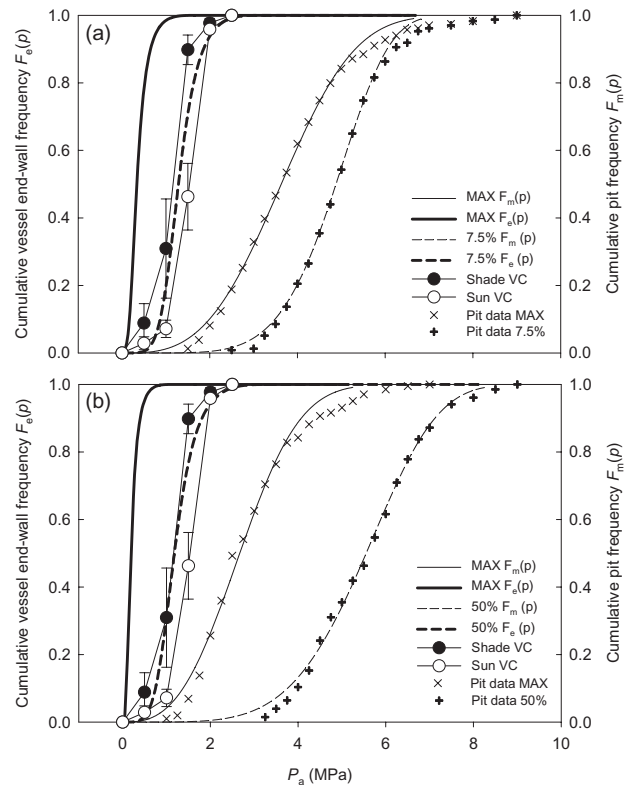

Figure 6. Fitted cumulative frequency distribution for the air-seeding pressure (P_a) of individual pits $[F_m(p)]$ and pitted end-walls $[F_e(p)]$ as calculated from the 'rare pit' model for ethanol-dried (a) and water-dried samples (b). The mean of the $F_e(p)$ distribution provides an estimate of the mean cavitation pressure (MCP). Results obtained when maximal pore diameter per individual pit was used to generate cumulative pit frequency distribution are shown together with the results providing reasonable agreement with measured MCP. This occurred when the average from 7.5 and 50% of the largest pore diameters per pit were used to generate $F_m(p)$ for ethanol- and water-dried samples, respectively. Closed and open circles show vulnerability curves from plants grown in shade and control light conditions, respectively.

Table 2. Fitted Weibull constants of empirical pit distributions and mean cavitation pressure from the 'rare pit' model for different pit pore diameter data

		Weibull parameters		
	D data	*b*	*c*	MCP_e (MPa)
Ethanol-dried	Max	4.08	3.14	−0.43
	1%	4.27	4.12	−0.73
	2.5%	4.59	4.76	−0.98
	5%	4.95	5.16	−1.18
	7.5%	5.21	5.61	−1.38
	10%	5.44	5.84	−1.52
Water-dried	Max	3.04	2.84	−0.27
	1%	3.19	3.23	−0.37
	10%	4.17	3.81	−0.63
	15%	4.48	3.99	−0.72
	30%	5.21	4.40	−0.98
	50%	5.99	4.83	−1.29

The *D* data column indicates what data was assumed as an empirical pit distribution (Max = the largest pore from an individual pit or the average from the indicated percentage of the largest pores per individual pit). *b* and *c* represent the Weibull parameters providing the best fit of Eqn 3 to empirical pit distribution data. MCP_e is mean end wall air-seeding pressure predicted by the model.

finding agrees with a recent study on angiosperm species, which found correlations between pit membrane thickness and membrane porosity as well as vulnerability to cavitation (Jansen *et al.* 2009). Species with thinner, more porous membranes should be more vulnerable than species with thicker membranes (Jansen *et al.* 2009), and such interspecific correlations may also occur within a single genotype. Thinner pit membranes in SH plants (Fig. 2a) probably represented a weaker barrier between air and water-filled vessels, and allowed air-seeding at lower ΔP_{crit} than in C plants with thicker pit membranes. The link between membrane porosity and thickness remained somewhat ambiguous in our study (Fig. 5), which may be caused by artefacts resulting from sample preparation (as discussed in the following). Several experiments have also suggested that pores become enlarged when the membrane deflects during air-seeding (Choat *et al.* 2004; Cochard *et al.* 2010). Such enlargement would presumably be more pronounced in the thinner membranes of SH plants and would contribute to the lower air-seeding threshold observed in SH plants, despite similar porosity under relaxed conditions. In any case, pit membrane thickness appears to be an important characteristic influencing cavitation resistance.

The factors determining pit membrane thickness are not fully understood. In this study, reduced pit membrane thickness in SH samples was paralleled by a thinner primary cell wall and middle lamella layer (Fig. 2b). As pit membranes are derived from this compound middle lamella, such a correlation is not unexpected. In shaded samples, there was no significant difference between the compound middle lamella and pit membrane thickness. In control samples, pit membranes were on average 50 nm thicker than the compound middle lamella. It is possible that some material

is deposited on the pit membrane surface as suggested by the observation that pit membranes were almost twice as thick as the compound middle lamella in some angiosperm species (Jansen *et al.* 2009).

The SEM-based measurements of pit porosity in SH and C samples produced different results depending on the sample preparation method (compare Fig. 4a,b, Fig. 5). When samples were water-dried (air-dried from water), pores appeared larger in SH than in C plants, which was in agreement with our initial hypothesis. However, there was no significant difference in pore sizes between SH and C when ethanol-drying was used. Consistent with the rare pit hypothesis, the vast majority (95%) of pores detected with SEM were smaller than the pore size allowing air-seeding at the *MCP*. This result is in agreement with previous SEM work (Choat *et al.* 2003). However, when we used the pit porosity data in the 'rare pit' model to predict *MCP*, the results suggested that pore sizes measured from SEM images overestimate real porosity (Table 2, Fig. 6),
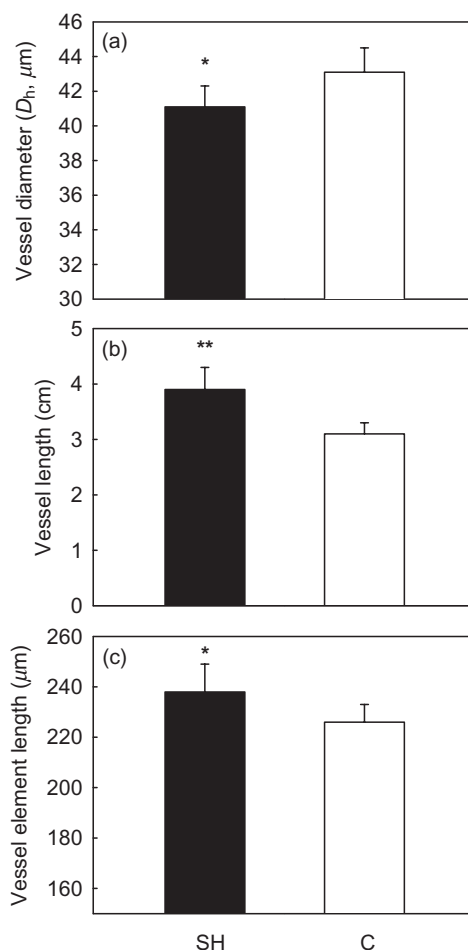
Figure 7. Mean hydraulic vessel diameter (a), mean vessel length (b) and mean vessel element length (c) in shaded (SH; black bars) and control plants (C; open bars). The bars represent grand means ± standard deviation from five to six individual stems. * and ** indicate significant differences at *P* < 0.05 and 0.01, respectively (independent two-sample *t*-test).
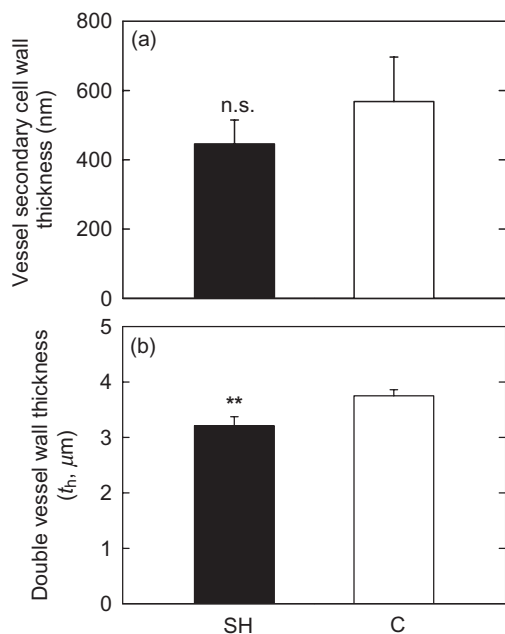
Figure 8. Secondary cell wall thickness in vessels measured from transmission electron microscopy (TEM) micrographs (a) and double vessel wall thickness measured with light microscopy (b). The bars represent grand means ± standard deviation ($n = 5$–6). ** indicates significant differences at $P < 0.01$ whereas n.s. indicates non-significant difference (independent two-sample *t*-test).

especially in the water-dried samples. There could be several possible reasons for this finding, and most likely a combination of them contributed to this result. First, sample dehydration may have resulted in a general enlargement of pores as the gelatinous material filling the space between the microfibrils shrank. It is possible that the effect of such shrinkage was more dramatic in thinner pit membranes, which might explain the larger porosity of water-dried samples in SH plants. Second, some of the large pores that we measured were probably artefacts or resulted from local damages to the membrane that were caused as some of the microfibrils ruptured during the desiccation process. Occasionally, some pores in an individual pit membrane were suspiciously larger than the rest of the pores, similar to the pattern found by Sano (2005, his Fig. 8). However, it was

difficult to draw a distinct line between pores that could be considered real and those resulting from artificial damage. The fact that model predictions based on the averages from 7.5% of the largest pores already provided a reasonable agreement with the measured *MCP* in ethanol-dried samples (Table 2) is encouraging as it indicates that the porosity measurements are relatively close to expected reality. Nonetheless, the exact magnitude of pore enlargement caused by the sample dehydration method is difficult to quantify because of the inherent difficulty of locating the rare pits with the largest pores thus measuring the real range of D_{max} values.

Based on our results from poplar xylem, ethanol dehydration seems to be a better alternative for preparing pit membrane samples for SEM-imaging in comparison with air-drying as it produced a higher number of intact pit membranes with more reasonable porosity. Air-drying from pure ethanol was presumably less disruptive than air-drying from water and hence, preserved pit membrane structure closer to its natural state. This finding contrasts with conclusions of Jansen *et al.* (2008) who got better results with water-drying of samples prior to SEM observations. It is possible that some preparation techniques are more suitable for certain species. Notably, Jansen *et al.* used species with thicker pit membranes than those found in poplar. Thicker membranes are probably more resistant to the negative effects of air-drying from water.

Although ethanol-drying provided better results, it was probably far from being free of artefacts. In a few instances, we observed a layer that tended to detach around the perimeter of the pit membrane, creating an apparent white ring as the edges of the layer rolled up (Fig. 4c). In several angiosperm species (e.g. *Goniorrhachis*, *Salix*, *Betula*), pit membranes were shown to consist of multiple layers of microfibrils that can be peeled off during the sample preparation (Schmid & Machado 1968; Sano 2005; Jansen *et al.* 2009). In contrast to these SEM studies, in our case this upper layer appeared amorphous with no visible fibrils. In addition, we observed several pits that displayed a homogenous surface texture with no resolvable pores and microfibrils. In a pioneering study using atomic force microscopy for investigating the structural properties of pit membranes, Pesacreta, Groom & Rials (2005) found a microfibrillar coating at the surface of pit membranes of *Sapium sebiferum*. The coating was homogenously thick

Table 3. Properties of xylem cells and wood density of poplar saplings grown under shade (SH) or control light conditions (C)

	Fibre diameter (µm)	Fibre length (µm)	Secondary cell wall thickness of fibres (nm)	Wood density (g cm⁻³)
SH	19.5 ± 0.9	531.1 ± 23.3	762.5 ± 65.3	0.32 ± 0.01
C	19.8 ± 0.8	580.7 ± 15.7	1031.6 ± 163.2	0.40 ± 0.01
P value	ns (0.540)	0.001	<0.01	<10⁻³

Diameter and length of fibres (measured from macerations, grand means of $n = 6$ stems), thickness of secondary cell wall of fibres (measured from transmission electron microscopy micrographs, grand means of $n = 5$ stems), and wood density ($n = 6$). Means ± standard deviation. P values show results of independent two-sample *t*-tests; ns = non-significant difference.

when non-dried samples were observed, while air-dried samples showed variability in the thickness of this coating. The coating was on average thinner when compared with non-dried samples. Thus, it is possible that the layer shown in Fig. 4c represents a similar coating. Although the chemical nature of this coating is not known, Pesacreta *et al.* suggested that polyphenolics or pectins might be present.

Strikingly, our TEM immunolabelling procedure using the antibodies JIM5 and JIM7 failed to detect HG in poplar pit membranes with a notable exception of the annulus region (Fig. 3a,b). These results should be verified in naturally grown mature poplar trees as it is possible that the young age of the seedlings influenced the chemical composition of the pit membranes and compound middle lamella. Nevertheless, the overall pattern of labelling in the compound middle lamella in our experiment was similar to the pattern found in mature wood of Scots pine (Hafren, Daniel & Westermark 2000). However, in the case of pine, the torus of the pit membrane was labelled as well. In poplar, the labelling suggests that HG were removed or modified when the compound middle lamella developed into a pit membrane. It has been suggested that non-cellulosic polysaccharides are hydrolysed in the pit membranes of *Salix* (O'Brien 1970). In a recent study, Herbette & Cochard (2010) showed that removal of calcium from the conduit cell wall resulted in increased xylem vulnerability in eleven tree species while no effect of calcium removal was found in *Salix* and *Betula*. The effect of calcium removal on vulnerability was attributed to the disruption of the supermolecular structure of HG polymers present in the pit membranes allowing air-seeding under less negative pressure. The absence of an effect of calcium removal on cavitation resistance in *Salix* and *Betula* suggests that HG might not be present in the pit membranes of these highly vulnerable species. In further support of our results, Nardini *et al.* (2007) did not find any differences in the ion-mediated effect on stem hydraulic conductivity in tobacco plants with reduced HG content when compared with control plants with unaltered composition. We suggest that the current paradigm about the general presence of HG in mature pit membranes needs to be reconsidered. To date, there is no *direct* evidence that pectins are present in mature angiosperm pit membranes (Choat *et al.* 2008), even though there is clear evidence for the occurrence of pectins in pit membranes of conifers (Hafren *et al.* 2000).

Some kind of filling material in which cellulosic microfibrils are embedded is clearly present but the question about its chemical nature remains unresolved. Given the dramatically different appearance of pit membranes in different species (Jansen *et al.* 2009), variability in their chemical composition may be expected. While HG may be present in the pit membranes of some species (Perez-Donoso *et al.* 2010), they may be absent or masked in other species like poplar, willow or birch. Hemicelluloses and two other groups of pectin (rhamnogalacturonan I and II) are commonly present in primary cell walls (Fry 2004), and are probably also present in pit membranes. In addition, Schmitz *et al.* (2008) reported a low but detectable lignin

content in pit membranes of two mangrove species. The presence of hydrophobic substances such as lignin in pit membrane would have an important effect on xylem vulnerability as a non-zero contact angle in Eqn 1 would result in a lower cavitation pressure for a given pore size (Meyra, Kuz & Zarragoicoechea 2007). More research addressing pit membrane chemistry is clearly required for a better understanding of inter-vessel pit functioning.

The xylem of SH grown poplars was not only more vulnerable, but also exhibited lower transport efficiency (Fig. 1b). These observations are in line with earlier results (Lemoine, Jacquemin & Granier 2002; Raimondo *et al.* 2009). Lower K_s can be explained by significantly narrower vessels found in SH plants (Fig. 7a). However, the vessels in SH plants were also longer (Fig. 7b), which should result in smaller end wall resistance as xylem sap crosses fewer end walls in series. This decrease in end wall resistance was probably not big enough to compensate for the effect of narrower vessels. The xylem of SH plants therefore appears less optimized from a hydraulic standpoint. This study also reinforces the point that higher xylem vulnerability is not always associated with increased xylem transport efficiency; especially when looking at the intraspecific level (Martinez-Vilalta *et al.* 2009; Fichot *et al.* 2010).

Despite smaller xylem areas and lower xylem transport efficiency, the total leaf area was comparable between SH and C plants (Table 1). This implies that K_L was lower in SH plants compared with their C counterparts (Fig. 1c). Lower K_L in plants growing under shade has been previously reported from both controlled and field conditions (Schultz & Matthews 1993; Caquet *et al.* 2009; Schoonmaker *et al.* 2010). In shade conditions, the vapour pressure difference between the leaf and ambient atmosphere is usually low. Well-watered plants can maintain large leaf areas even though their xylem transport is less efficient. A large leaf area in shade is desirable as it helps to capture more light, which represents the main limiting factor in such an environment. However, low K_L can represent a risk to the plant under high evaporative demands as insufficient water supply to the leaves may result in stomatal closure and/or xylem cavitation.

As obvious from lower wood densities and thinner cell walls in both vessels and fibres (Fig. 8a,b, Table 3), the mechanical function of xylem was suppressed in SH plants, probably because of limiting carbon availability. The lower wood density in SH plants was driven mainly by the lower fibre cell wall thickness, because the diameter of fibres as well as vessel density were not significantly different between SH and C plants. It is also worth noticing that the fibre length was lower in SH plants (Table 2), which contrasts with the pattern found with vessel and vessel element length. During xylogenesis, the future vessel elements and fibres have the same length until an intensive intrusive growth of fibre tips is initiated (Siedlecka *et al.* 2008). Hence, our data suggest that the intrusive growth of fibres was inhibited in SH plants relative to C. Consistent with our results, lower wood density (Hacke *et al.* 2001) and decreased double wall thickness (Cochard *et al.* 2008) are often associated with

increased xylem vulnerability. The link between these characteristics and xylem safety has been viewed as indirect and based on the fact that strong mechanical reinforcement is required in cavitation-resistant conduits to prevent their collapse when they are subjected to highly negative xylem pressure (Hacke *et al.* 2001). However, there may be a coordination between compound middle lamella (and hence pit membrane) thickness and overall cell wall thickness, which could influence wood density as suggested by Jansen *et al.* (2009). The results presented in this study (Fig. 2) are in agreement with their hypothesis. However, more research is required to further verify this proposed link between wood density and xylem vulnerability.

In conclusion, this study provides new insights into homogenous pit membrane functioning. The results presented here indicate that the structure of homogenous pit membranes in poplar is affected by growing conditions. The thinner pit membranes that developed in SH plants served as a weaker protection against air-seeding resulting in more vulnerable xylem. By using the empirical pit porosity data in conjunction with the 'rare pit' model we were able to evaluate how SEM-based porosity estimates compared with the porosity expected based on the air-seeding theory. To the best of our knowledge, this is the first study using carbohydrate-specific antibodies to dissect intervessel pit membrane chemistry in poplar. Pectic HG are believed to be responsible for many physiological processes associated with pit functioning such as the ion-mediated changes in hydraulic conductivity or calcium-dependant changes in xylem vulnerability. Our finding that HG are not universally present in all angiosperm pit membranes highlights the need for a better characterization of pit membrane structure and function.

ACKNOWLEDGMENTS

REFERENCES

Alder N.N., Pockman W.T., Sperry J.S. & Nuismer S. (1997) Use of centrifugal force in the study of xylem cavitation. *Journal of Experimental Botany* **48,** 665–674.

Barigah T.S., Ibrahim T., Bogard A., Faivre-Vuillin B., Lagneau L.A., Montpied P. & Dreyer E. (2006) Irradiance-induced plasticity in the hydraulic properties of saplings of different temperate broad-leaved forest tree species. *Tree Physiology* **26,** 1505–1516.

Caquet B., Barigah T.S., Cochard H., Montpied P., Collet C., Dreyer E. & Epron D. (2009) Hydraulic properties of naturally regenerated beech saplings respond to canopy opening. *Tree Physiology* **29,** 1395–1405.

Choat B., Ball M., Luly J. & Holtum J. (2003) Pit membrane porosity and water stress-induced cavitation in four co-existing dry rainforest tree species. *Plant Physiology* **131,** 41–48.

Choat B., Cobb A.R. & Jansen S. (2008) Structure and function of bordered pits: new discoveries and impacts on whole-plant hydraulic function. *The New Phytologist* **177,** 608–625.

Choat B., Jansen S., Zwieniecki M.A., Smets E. & Holbrook N.M. (2004) Changes in pit membrane porosity due to deflection and stretching: the role of vestured pits. *Journal of Experimental Botany* **55,** 1569–1575.

Christman M.A., Sperry J.S. & Adler F.R. (2009) Testing the 'rare pit' hypothesis for xylem cavitation resistance in three species of *Acer. The New Phytologist* **182,** 664–674.

Cochard H., Barigah S.T., Kleinhentz M. & Eshel A. (2008) Is xylem cavitation resistance a relevant criterion for screening drought resistance among *Prunus* species? *Journal of Plant Physiology* **165,** 976–982.

Cochard H., Cruiziat P. & Tyree M.T. (1992) Use of positive pressures to establish vulnerability curves: further support for the air-seeding hypothesis and implications for pressure-volume analysis. *Plant Physiology* **100,** 205–209.

Cochard H., Herbette S., Hernandez E., Holtta T. & Mencuccini M. (2010) The effects of sap ionic composition on xylem vulnerability to cavitation. *Journal of Experimental Botany* **61,** 275–285.

Cochard H., Lemoine D. & Dreyer E. (1999) The effects of acclimation to sunlight on the xylem vulnerability to embolism in *Fagus sylvatica* L. *Plant, Cell & Environment* **22,** 101–108.

Domec J.C., Lachenbruch B., Meinzer F.C., Woodruff D.R., Warren J.M. & McCulloh K.A. (2008) Maximum height in a conifer is associated with conflicting requirements for xylem design. *Proceedings of the National Academy of Sciences of the United States of America* **105,** 12069–12074.

Fichot R., Barigah T.S., Chamaillard S., Le Thiec D., Laurans F., Cochard H. & Brignolas F. (2010) Common trade-offs between xylem resistance to cavitation and other physiological traits do not hold among unrelated *Populus deltoides* x *Populus nigra* hybrids. *Plant, Cell & Environment* **33,** 1553–1568.

Fry S.C. (2004) Primary cell wall metabolism: tracking the careers of wall polymers in living plant cells. *The New Phytologist* **161,** 641–675.

Goldberg R., Morvan C. & Roland J.C. (1986) Composition, properties and localization of pectins in young and mature cells of the mung bean hypocotyl. *Plant & Cell Physiology* **27,** 417–429.

Guglielmino N., Liberman M., Jauneau A., Vian B., Catesson A.M. & Goldberg R. (1997) Pectin immunolocalization and calcium visualization in differentiating derivatives from poplar cambium. *Protoplasma* **199,** 151–160.

Guillemin F., Guillon F., Bonnin E., Devaux M.F., Chevalier T., Knox J.P., Liners F. & Thibault J.F. (2005) Distribution of pectic epitopes in cell walls of the sugar beet root. *Planta* **222,** 355–371.

Hacke U.G., Plavcová L., Almeida-Rodriguez A., King-Jones S., Zhou W. & Cooke J.E.K. (2010) Influence of nitrogen fertilization on xylem traits and aquaporin expression in stems of hybrid poplar. *Tree Physiology* **30,** 1016–1025.

Hacke U.G., Sperry J.S., Pockman W.T., Davis S.D. & McCulloh K.A. (2001) Trends in wood density and structure are linked to prevention of xylem implosion by negative pressure. *Oecologia* **126,** 457–461.

Hafren J., Daniel G. & Westermark U. (2000) The distribution of acidic and esterified pectin in cambium, developing xylem and mature xylem of *Pinus sylvestris*. *Iawa Journal* **21,** 157–168.

Hafren J. & Westermark U. (2001) Distribution of acidic and esterified polygalacturonans in sapwood of spruce, birch and aspen. *Nordic Pulp & Paper Research Journal* **16,** 284–290.

Hargrave K.R., Kolb K.J., Ewers F.W. & Davis S.D. (1994) Conduit diameter and drought-induced embolism in *Salvia mellifera* Greene (Labiatae). *The New Phytologist* **126,** 695–705.

Herbette S. & Cochard H. (2010) Calcium is a major determinant of xylem vulnerability to cavitation. *Plant Physiology* **153,** 1932–1939.

Holste E.K., Jerke M.J. & Matzner S.L. (2006) Long-term acclimatization of hydraulic properties, xylem conduit size, wall strength and cavitation resistance in *Phaseolus vulgaris* in response to different environmental effects. *Plant, Cell & Environment* **29,** 836–843.

Jansen S., Choat B. & Pletsers A. (2009) Morphological variation of intervessel pit membranes and implications to xylem function in angiosperms. *American Journal of Botany* **96,** 409–419.

Jansen S., Pletsers A. & Sano Y. (2008) The effect of preparation techniques on SEM-imaging of pit membranes. *Iawa Journal* **29,** 161–178.

Knox J.P., Linstead P.J., King J., Cooper C. & Roberts K. (1990) Pectin esterification is spatially regulated both within cell walls and between developing tissues of root apices. *Planta* **181,** 512–521.

Lemoine D., Jacquemin S. & Granier A. (2002) Beech (*Fagus sylvatica* L.) branches show acclimation of xylem anatomy and hydraulic properties to increased light after thinning. *Annals of Forest Science* **59,** 761–766.

Martinez-Vilalta J., Cochard H., Mencuccini M., *et al.* (2009) Hydraulic adjustment of Scots pine across Europe. *The New Phytologist* **184,** 353–364.

McDowell N., Pockman W.T., Allen C.D., *et al.* (2008) Mechanisms of plant survival and mortality during drought: why do some plants survive while others succumb to drought? *The New Phytologist* **178,** 719–739.

Meyra A.G., Kuz V.A. & Zarragoicoechea G.J. (2007) Geometrical and physicochemical considerations of the pit membrane in relation to air seeding: the pit membrane as a capillary valve. *Tree Physiology* **27,** 1401–1405.

Micheli F., Ermel F.F., Bordenave M., Richard L. & Goldberg R. (2002) Cell walls of woody tissues: cytochemical, biochemical and molecular analysis of pectins and pectin methylesterases. In *Wood Formation in Trees: Cell and Molecular Biology Techniques* (ed. N.J. Chaffey), pp. 179–200. Taylor & Francis, London.

Nardini A., Gasco A., Cervone F. & Salleo S. (2007) Reduced content of homogalacturonan does not alter the ion-mediated increase in xylem hydraulic conductivity in tobacco. *Plant Physiology* **143,** 1975–1981.

O'Brien T.P. (1970) Further observations on hydrolysis of the cell wall in the xylem. *Protoplasma* **69,** 1–14.

Perez-Donoso A.G., Sun Q., Roper M.C., Greve L.C., Kirkpatrick B. & Labavitch J.M. (2010) Cell wall-degrading enzymes enlarge the pore size of intervessel pit membranes in healthy and *Xylella fastidiosa*-infected grapevines. *Plant Physiology* **152,** 1748–1759.

Pesacreta T.C., Groom L.H. & Rials T.G. (2005) Atomic force microscopy of the intervessel pit membrane in the stem of *Sapium sebiferum* (Euphorbiaceae). *Iawa Journal* **26,** 397–426.

Raimondo F., Trifilo P., Lo Gullo M.A., Buffa R., Nardini A. & Salleo S. (2009) Effects of reduced irradiance on hydraulic architecture and water relations of two olive clones with different growth potentials. *Environmental and Experimental Botany* **66,** 249–256.

Sano Y. (2005) Inter- and intraspecific structural variations among intervascular pit membranes as revealed by field-emission scanning electron microscopy. *American Journal of Botany* **92,** 1077–1084.

Schmid R. & Machado R.D. (1968) Pit membranes in hardwoods – Fine structure and development. *Protoplasma* **66,** 185–204.

Schmitz N., Koch G., Schmitt U., Beeckman H. & Koedam N. (2008) Intervessel pit structure and histochemistry of two mangrove species as revealed by cellular UV microspectrophotometry and electron microscopy: intraspecific variation and functional significance. *Microscopy and Microanalysis* **14,** 387–397.

Schoonmaker A.L., Hacke U.G., Landhausser S.M., Lieffers V.J. & Tyree M.T. (2010) Hydraulic acclimation to shading in boreal conifers of varying shade tolerance. *Plant, Cell & Environment* **33,** 382–393.

Schultz H.R. & Matthews M.A. (1993) Xylem development and hydraulic conductance in sun and shade shoots of grapevine (*Vitis vinifera* L.) – Evidence that low-light uncouples water transport capacity from leaf area. *Planta* **190,** 393–406.

Shane M.W., McCully M.E. & Canny M.J. (2000) Architecture of branch-root junctions in maize: structure of the connecting xylem and the porosity of pit membranes. *Annals of Botany* **85,** 613–624.

Shumway D.L., Steiner K.C. & Kolb T.E. (1993) Variation in seedling hydraulic architecture as a function of species and environment. *Tree Physiology* **12,** 41–54.

Siedlecka A., Wiklund S., Peronne M.A., Micheli F., Lesniewska J., Sethson I., Edlund U., Richard L., Sundberg B. & Mellerowicz E.J. (2008) Pectin methyl esterase inhibits intrusive and symplastic cell growth in developing wood cells of *Populus*. *Plant Physiology* **146,** 554–565.

Sperry J.S. (2000) Hydraulic constraints on plant gas exchange. *Agricultural and Forest Meteorology* **2831,** 1–11.

Sperry J.S., Hacke U.G. & Wheeler J.K. (2005) Comparative analysis of end wall resistivity in xylem conduits. *Plant, Cell & Environment* **28,** 456–465.

Sperry J.S., Saliendra N.Z., Pockman W.T., Cockhard H., Cruiziat P., Davis S.D., Ewers F.W. & Tyree M.T. (1996) New evidence for large negative xylem pressures and their measurement by the pressure chamber method. *Plant, Cell & Environment* **19,** 427–436.

Sperry J.S. & Tyree M.T. (1988) Mechanism of water stress-induced xylem embolism. *Plant Physiology* **88,** 581–587.

Stiller V. (2009) Soil salinity and drought alter wood density and vulnerability to xylem cavitation of baldcypress (*Taxodium distichum* (L.) Rich.) seedlings. *Environmental and Experimental Botany* **67,** 164–171.

Tyree M.T. & Zimmermann M.H. (2002) *Xylem Structure and the Ascent of Sap* 2nd edn, Springer Verlag, Berlin.

Wheeler J.K., Sperry J.S., Hacke U.G. & Hoang N. (2005) Intervessel pitting and cavitation in woody Rosaceae and other vesselled plants: a basis for a safety versus efficiency trade-off in xylem transport. *Plant, Cell & Environment* **28,** 800–812.

Willats W.G.T., McCartney L., Mackie W. & Knox J.P. (2001) Pectin: cell biology and prospects for functional analysis. *Plant Molecular Biology* **47,** 9–27.

Zwieniecki M.A., Melcher P.J. & Holbrook N.M. (2001) Hydrogel control of xylem hydraulic resistance in plants. *Science* **291,** 1059–1062.